



# In vitro studies of $^{223}\text{Ra}$ - and $^{225}\text{Ac}$ -labelled $\alpha$ -zirconium phosphate as potential carrier for alpha targeted therapy

Michal Sakmár<sup>1</sup> · Lukáš Ondrák<sup>1</sup> · Kateřina Fialová<sup>1</sup> · Martin Vlk<sup>1</sup> · Ján Kozempel<sup>1</sup> · Frank Bruchertseifer<sup>2</sup> · Alfred Morgenstern<sup>2</sup>

Received: 24 June 2022 / Accepted: 22 December 2022 / Published online: 14 January 2023  
© The Author(s) 2023

## Abstract

In this study suitability of  $\alpha$ -ZrP nanoparticles as a  $^{223}\text{Ra}$  and  $^{225}\text{Ac}$  carriers for TAT was investigated. The yields of radiolabelling were higher than 98% in both cases. Subsequently, in vitro stability studies were carried out in various biological matrices during 48 h period. Measurements of released radioactivity showed the highest stability in saline. Released activity of  $^{223}\text{Ra}$ ,  $^{225}\text{Ac}$  and their daughter radionuclides was around 0.5%. On the other hand, the lowest stability was shown in plasma and serum. Released activity for  $^{223}\text{Ra}$ ,  $^{225}\text{Ac}$  and their progeny atoms was from 15 to 32%.

**Keywords** Targeted alpha therapy ·  $^{223}\text{Ac}$  ·  $^{223}\text{Ra}$  · Recoil atoms · Stability studies

## Introduction

Targeted alpha particle therapy (TAT) is one of the promising possibilities for the treatment of a broad range of malignancies. Due to the short range of alpha particles in soft tissue, alpha particles can destroy tumours effectively while causing only little damage to surrounding healthy tissue. The range of the alpha particle through the tissue is generally limited to few micrometers (50–100), which corresponds to maximum of six cell diameters. In addition, the emitted alpha particles are highly energetic and the passage of these particles through the tissue is associated with high linear energy transfer (LET) of 50–230 keV/ $\mu\text{m}$  [1]. The high LET of alpha particles leads to the efficient cell destruction through high ionization rates and clusters of DNA double-strand breaks. These breaks are very difficult to repair and often lead to cell cycle arrest followed by mitotic cell death, apoptosis or necrosis [2]. Currently, there are only few such radionuclides that are suitable for usage in nuclear medicine.

Two widely investigated radionuclides,  $^{223}\text{Ra}$  ( $T_{1/2} = 11.4$  d) and  $^{225}\text{Ac}$  ( $T_{1/2} = 9.9$  d), are among the most promising ones for targeted alpha particle therapy [3].

Many alpha radionuclides, including  $^{223}\text{Ra}$  and  $^{225}\text{Ac}$ , decay by a cascade of alpha particles (Figs. 1, 2), which can increase TAT performance but also contribute to the irradiation of non-target tissues if the daughter atoms recoil and have a chance to leave the site of origin [4]. Nanoparticles can serve as suitable radionuclide carriers for TAT, particularly considering their ability to, at least partially, stop the progeny recoils spread and keep them immobilised in their structure. At the same time these nanoparticles can be surface-modified, which may improve their targeting, stability and other biological and chemical properties [5, 6]. In nuclear medicine, many types of nanoparticles based on organic or inorganic substances have been tested as suitable carriers for alpha emitters.

Various nanoparticles (NPs) including  $\text{TiO}_2$  [7] Hydroxyapatite [7], SPIONs [8], Nanozeolite A [9] or reduced graphite oxide [10] were labelled with  $^{223}\text{Ra}$ . In these studies, radionuclide immobilisation and release activity of  $^{223}\text{Ra}$  were monitored. Bilewicz et al. [11] prepared composite nanoparticles consisting of trastuzumab-surface-modified barium ferrite. They studied the affinity of prepared composite to breast and ovarian cancer cells (SKOV-3).

The other potential alpha radionuclide for use in nuclear medicine is  $^{225}\text{Ac}$ . In order to stop the release of daughter atoms, systems containing nanoparticles have also

✉ Michal Sakmár  
msakmar26@gmail.com

<sup>1</sup> Department of Nuclear Chemistry, Faculty of Nuclear Sciences and Physical Engineering, Czech Technical University in Prague, Břehová 7, 115 19 Prague 1, Czech Republic

<sup>2</sup> Joint Research Centre, European Commission, Karlsruhe, Germany

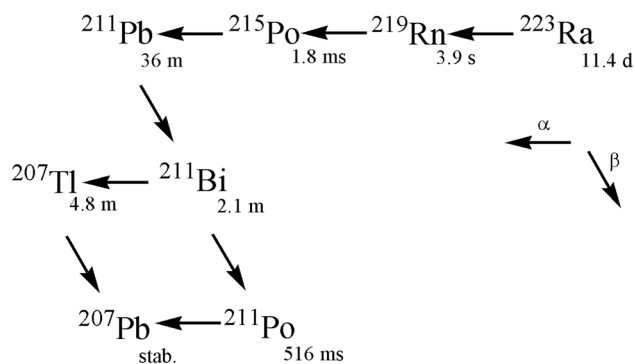


Fig. 1 Decay scheme of  $^{223}\text{Ra}$

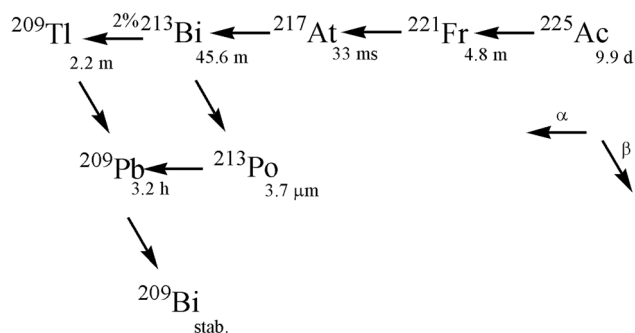


Fig. 2 Decay scheme of  $^{225}\text{Ac}$

been proposed as carriers. Several organic NPs based on liposomes or polymers which have been modified with antigens or antibodies have been tested [12, 13]. Inorganic substances like Au NPs [14],  $\text{TiO}_2$  [15],  $\text{La}(^{225}\text{Ac})\text{PO}_4$  [16], gadolinium vanadate [17] or carbon nanotubes [18] have been studied. The latter nanotubes were also coated with suitable antibodies and the in vitro affinity to tumor cells was observed.

The aim of this work is to verify the suitability of using alpha zirconium phosphate ( $\alpha$ -ZrP) nanoparticles as a carrier for alpha emitters. Nanoparticles of  $\alpha$ -ZrP are biocompatible and non-toxic material that can be used as a drug delivery system [19]. This work studies the sorption of radionuclides  $^{223}\text{Ra}$  and  $^{225}\text{Ac}$  onto the surface of  $\alpha$ -ZrP nanoparticles and the subsequent in vitro studies focused on measuring the released activity in selected biological matrices.

## Experimental

### Materials

All used chemicals were of analytical grade and were used without further purification. Zirconium oxychloride

octahydrate, sodium dihydrogen phosphate, hydrochloric acid were purchased from Merck (Darmstadt, Germany). Solution for in vitro studies: bovine serum, bovine plasma and lyophilised albumin (pH 7) were bought from Biowest (Nuaillé, France). For separation of samples VWR Micro Star 12 centrifuge was used (VWR International, Radnor, PA, USA). The hydrodynamic size distributions of studied particles and zeta potential were determined using dynamic light scattering (Nano-ZS, ZEN 3600, Malvern). Radium-223 was obtained as  $^{223}\text{RaCl}_2$  (Bayer Pharma AG) and actinium-225 as  $^{225}\text{Ac}(\text{NO}_3)_3$  separated from  $^{229}\text{Th}$  source (Karlsruhe, Germany).

### Preparation of $\alpha$ -ZrP

Nanoparticles of  $\alpha$ -ZrP were prepared by the reaction of zirconium oxychloride octahydrate aqueous solution with sodium dihydrogen phosphate solution in hydrochloric acid under the reflux according to Ondrák et al. [20]. The prepared particles were washed and suspended in ultrapure water. The size of  $\alpha$ -ZrP was determined using dynamic light scattering (DLS) method and the  $\zeta$ -potentials were also measured.

### Labelling procedure and in vitro studies

The radiolabelling was performed by surface sorption of  $^{223}\text{Ra}$  and  $^{225}\text{Ac}$  on the prepared  $\alpha$ -ZrP in saline. At the beginning, 6 mg of  $\alpha$ -ZrP were suspended in 0.5 ml of saline, then a solution containing approx. 100–300 kBq of  $^{223}\text{RaCl}_2$  or  $^{225}\text{Ac}(\text{NO}_3)_3$  was added. The added activity was measured by ionization chamber (PTW Curiemeter, Germany) and samples were stirred at laboratory temperature. Prepared  $^{223}\text{Ra}[\text{ZrP}]$  or  $^{225}\text{Ac}[\text{ZrP}]$  nanoparticles were centrifugated and washed by 0.5 ml fresh solution of saline (3x).

### In vitro stability of $^{223}\text{Ra}[\text{ZrP}]$ or $^{225}\text{Ac}[\text{ZrP}]$

Subsequent in vitro stability studies were carried out in bovine serum, bovine plasma, saline and 5% albumin solution. Radiolabelled NPs were centrifugated, the saline solution was removed, and 1 ml of the studied biological matrices was added. During 48 h period, samples were incubated at room temperature and mixing. After 1; 3; 6; 9; 12; 24 and 48 h, the samples were centrifugated and 0.5 ml of solution was measured on HPGe gamma spectrometer (Ortec, USA) which was calibrated with  $^{133}\text{Ba}$   $^{241}\text{Am}$   $^{137}\text{Cs}$  and  $^{152}\text{Eu}$  standards in a volume of 1 ml (distance S-D=0). Spectra were acquired and evaluated by Maestro software using nuclear data from the Nudat 3 library [21]. The measured solution was then returned to the nanoparticles and the sample was suspended and stirred again. Released activity was calculated from the gamma spectra by comparing the

**Table 1** Particles size and  $\zeta$ -potential measured by DLS

Particle size (nm)	$\zeta$ -Potential (mV)
105 ± 15	− 37.2 ± 3.1

activity of the removed solution and the activity of the nanoparticles in solution at the beginning of the experiments. The released activities of  $^{221}\text{Fr}$  and  $^{213}\text{Bi}$  from  $^{225}\text{Ac}$  and  $^{211}\text{Pb}$  and  $^{211}\text{Bi}$  from  $^{223}\text{Ra}$  were monitored. Measured data were corrected for decay. All in vitro experiments were performed in laminar box Airflow 150 UV (Esi FLUFRANCE, Arcueil, France). All in vitro studies with  $^{223}\text{Ra}$ ]ZrP or  $^{225}\text{Ac}$ ]ZrP were performed three times and uncertainties of release activity were calculated using standard deviation.

## Results and discussion

### Preparation of $\alpha$ -ZrP

The prepared  $\alpha$ -ZrP nanoparticles were fully characterized by Ondrak et al. [22] and the obtained results corresponded to the data reported in the libraries. Before the radiolabelling of prepared nanoparticles, the size of particles and  $\zeta$ -potential were measured using DLS (Table 1).

The measured data show that the average particle size was slightly larger than 100 nm which is the upper limit given for nanoparticle size. On the other hand, the  $\zeta$ -potential shows that the prepared nanoparticles were stable in solution and did not aggregate (Stable particles are those whose zetapotential is either below − 30 mV or above 30 mV). Due to the high stability in solution and only a slight deviation from the required particle size, these particles were chosen as suitable for further experiments with radionuclides  $^{223}\text{Ra}$  and  $^{225}\text{Ac}$ .

### Radiolabelling

The yield of radiolabelling was calculated according to Eq. (1).

$$Y\% = (A_{\text{NPs}}/A_{\text{int}}) \times 100 \quad (1)$$

In Eq. (1)  $Y\%$  represent the yield,  $A_{\text{NPs}}$  is the final activity of nanoparticles after being three-times washed by saline and  $A_{\text{int}}$  is the initial activity of  $^{223}\text{Ra}$  or  $^{225}\text{Ac}$ . Yields of radiolabelling are shown in Table 2. Measurement errors in Table 2 were calculated using standard deviation.

Based on these results, both radionuclides are strongly anchored on the surface of the nanoparticles during preparation. The measured gamma spectra of the removed solutions over the centrifuged particles showed that the released activity belonged just to decay products of  $^{223}\text{Ra}$  and  $^{225}\text{Ac}$ .

**Table 2** Yields of radiolabelling of  $\alpha$ -ZrP nanoparticles;  $n = 5$ 

Radionuclides	$^{223}\text{Ra}$	$^{225}\text{Ac}$
Yields (%)	98.5 ± 0.9	98.1 ± 1.2

### In vitro stability studies of radiolabeled $\alpha$ -ZrP

These experiments were performed in a system that was stirred thoroughly and the recoiled daughter atoms were allowed to be reabsorbed onto the surface of the nanoparticles. The prepared system was considered stable, if the released activity of  $^{223}\text{Ra}$  and  $^{225}\text{Ac}$  and their daughter products was during the incubation period in all biological matrices under 5%. Stability studies of both systems  $^{223}\text{Ra}$ ]ZrP and  $^{225}\text{Ac}$ ]ZrP were carried out for 48 h in saline, bovine serum, bovine plasma and 5% solution of albumine.

The percentage of the released activity for each studied radionuclide was calculated from the modified Eq. (1), where  $A_{\text{NPs}}$  was replaced by  $A_{\text{s}(x)}$  indicating the activity of the particular radionuclide in the removed solution and  $A_{\text{int}}$  was replaced by  $A_{\text{int}(x)}$  indicating the activity of the given radionuclide in the nanoparticle solution at the beginning of the experiment. The value of  $A_{\text{int}(x)}$  was measured when the parent radionuclides  $^{223}\text{Ra}$  and  $^{225}\text{Ac}$  were in equilibrium with their daughter products  $^{211}\text{Pb}$ ,  $^{211}\text{Bi}$  and  $^{221}\text{Fr}$ ,  $^{213}\text{Bi}$ .

In vitro stability studies of  $^{223}\text{Ra}$ ]ZrP are shown in Fig. 3. As can be seen the percentage of the released activity varies for each biological matrix. As expected, the radiolabelled nanoparticles are most stable in saline, where only less than 1.5% of  $^{223}\text{Ra}$  was released during the entire 48 h period. On the other hand, the lowest stability was observed in plasma, where up to 14% of  $^{223}\text{Ra}$  was released. From the obtained data, it can be seen that the released activity of the daughter atoms  $^{211}\text{Pb}$  and  $^{211}\text{Bi}$  is the same as released activity of  $^{223}\text{Ra}$ . However, significant difference can be seen in case of the bovine serum studies, where the difference between released activity of  $^{223}\text{Ra}$  and its daughter products is up to 10 percentage points. The same trend was also observed in bovine plasma; however, differences were smaller and later the values balanced out. These differences occur probably due to easier resorption of daughter atoms in biological matrices which have lower density (saline, albumin), as well as stabilization and envelopment of daughter atoms by the protein in serum and plasma, preventing weak resorption back to the surface of the nanoparticles.

Activities washout from  $\alpha$ -ZrP NPs labelled with  $^{225}\text{Ac}$  are shown in Fig. 4. As well as the  $^{223}\text{Ra}$ -labeled nanoparticles, the lowest released activity of  $^{225}\text{Ac}$  was measured in saline (lower than 0.5%) and the highest in blood serum (around 15%). However, as can be seen, the stability of  $^{225}\text{Ac}$ ]ZrP is lower in biological matrices (except the saline), than in the case of  $^{223}\text{Ra}$ ]ZrP. Another important

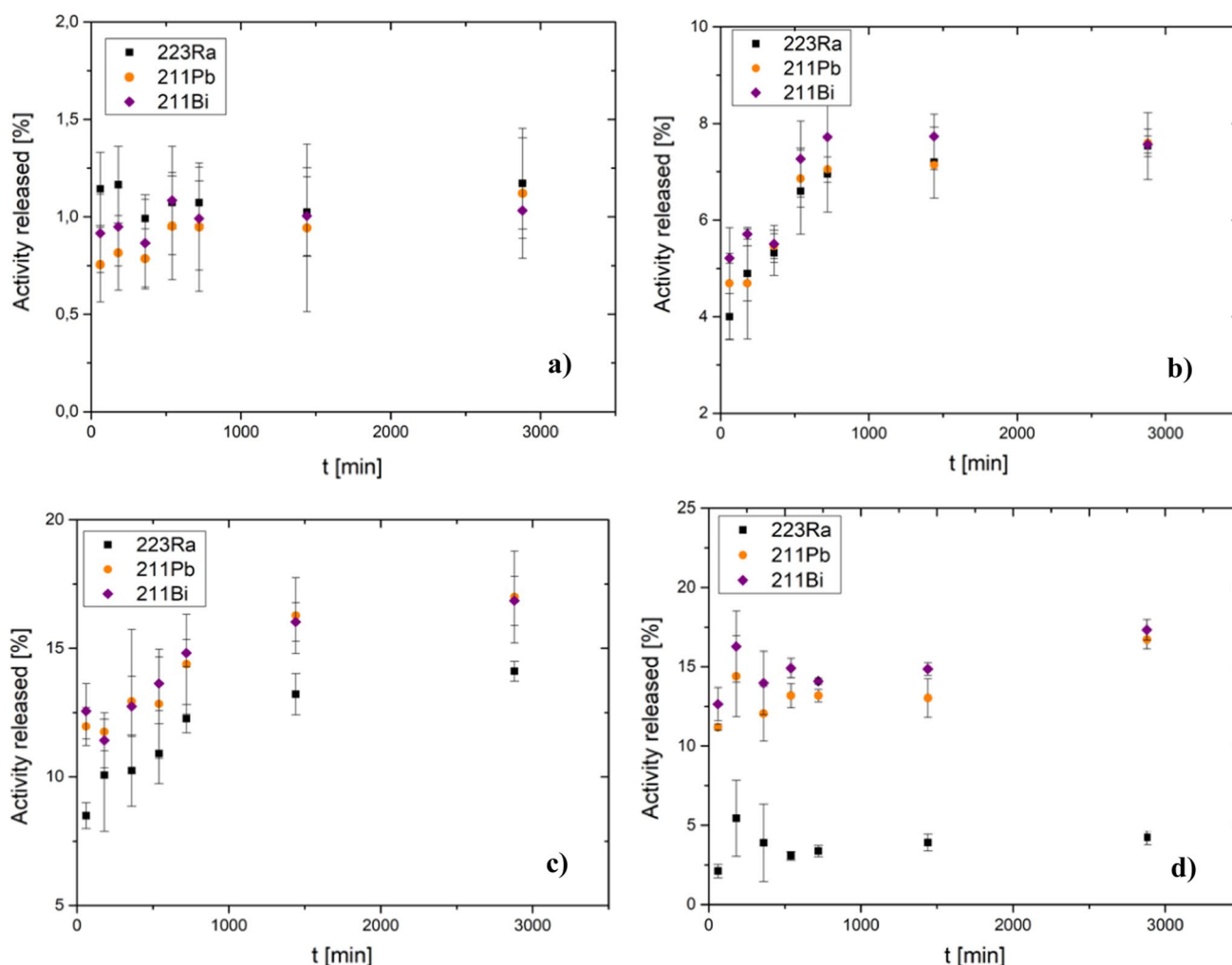


**Fig. 3** In vitro stability study of  $^{223}\text{Ra}$ -labelled nanoparticles of  $\alpha\text{-ZrP}$  **a** in saline, **b** 5% solution of albumin, **c** bovine plasma, **d** bovine serum

conclusion is that the difference between the released activity of  $^{225}\text{Ac}$  and its daughter product  $^{213}\text{Bi}$  is above 10 percentage points. In the bovine serum is difference up to 20 percentage points. On the other hand, maximal  $^{221}\text{Fr}$  released activity is 2 percentage points higher than that of  $^{225}\text{Ac}$  (albumin solution). These differences might be caused by the fact that  $^{221}\text{Fr}$  is the first decay product of  $^{225}\text{Ac}$ , it does not migrate long range in biological matrices and can be resorbed to the surface of the particles.

Comparing Figs. 3 and 4, it can be seen that the released activity [ $^{225}\text{Ac}$ ]ZrP is higher in all biological matrices (except saline), compared to [ $^{223}\text{Ra}$ ]ZrP. The variations in the growth of the released activity over time as mentioned above may be due to the resorption of the radionuclide onto the nanoparticles surface. The resorption can be caused by the fact that after the measurement of the activity of supernatant it was returned to the original solution with NPs. This theory could be verified by designing

a system where a biological matrix would flow around the nanoparticles to prevent resorption.

## Conclusions

The prepared  $\alpha\text{-ZrP}$  nanoparticles showed high sorption rate of Ra and Ac-radionuclides to their surface. The radiochemical yield was above 98% for both radionuclides. During in vitro studies in various biological matrices, released activity of  $^{223}\text{Ra}$  and  $^{225}\text{Ac}$  was measured together with some of their daughter progeny such as  $^{211}\text{Pb}$ ,  $^{211}\text{Bi}$  and  $^{221}\text{Fr}$ ,  $^{213}\text{Bi}$  respectively. From the obtained data it can be seen that the released activity was the highest in plasma and serum for both [ $^{225}\text{Ac}$ ]ZrP and [ $^{223}\text{Ra}$ ]ZrP systems. Released activity from  $^{223}\text{Ra}$  was about 10% and similar results were obtained for  $^{225}\text{Ac}$ . Larger differences were observed in the released activity of the daughter products:

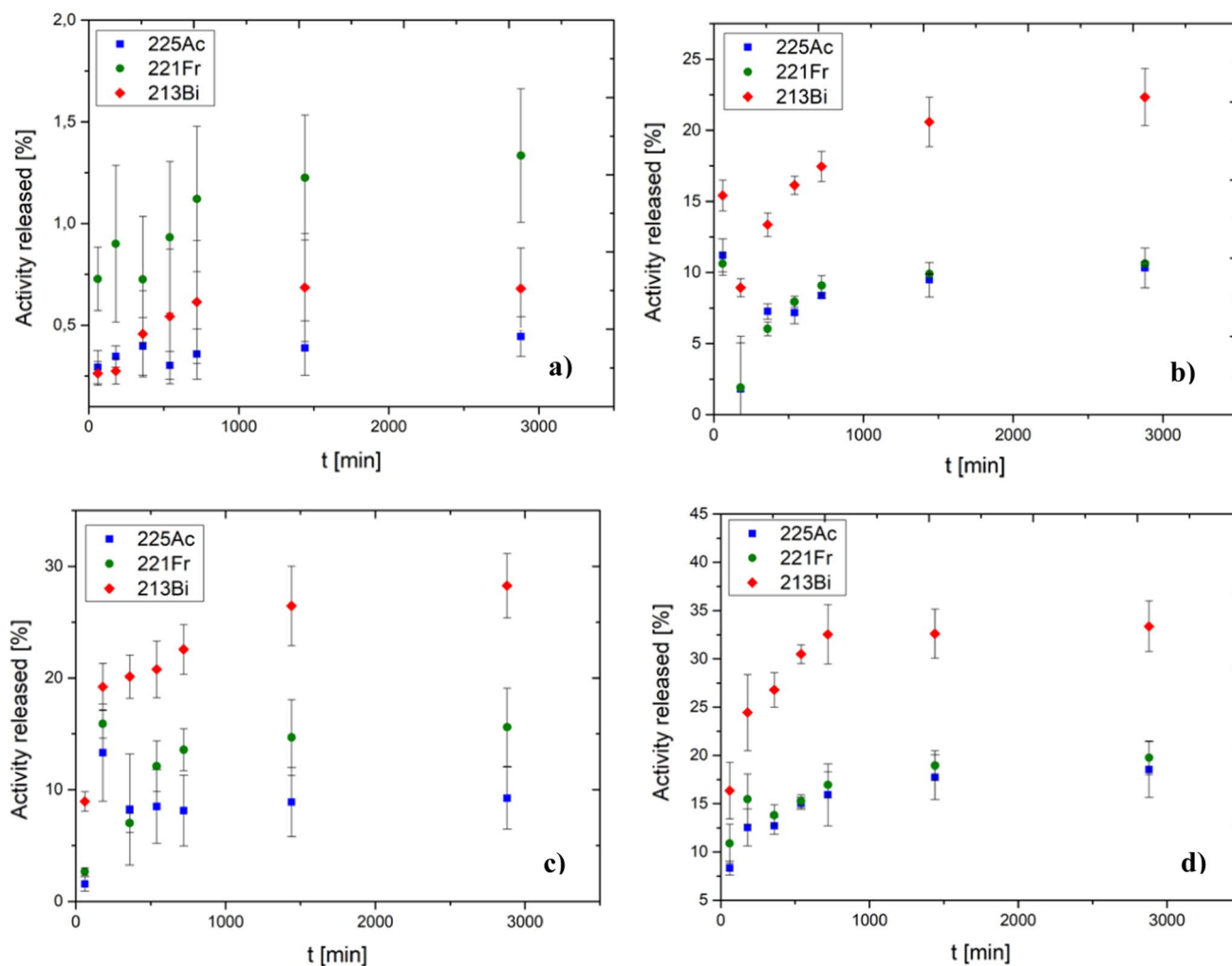


**Fig. 4** In vitro stability study of  $^{225}\text{Ac}$ -labelled nanoparticles of  $\alpha\text{-ZrP}$  **a** in saline, **b** 5% solution of albumin, **c** bovine plasma, **d** bovine serum

the decay products  $^{211}\text{Pb}$  and  $^{211}\text{Bi}$  had similar released activities as their parent radionuclide  $^{223}\text{Ra}$ . The exception was blood serum where the release was 5% from  $^{223}\text{Ra}$  and approximately 15% from  $^{211}\text{Pb}$  and  $^{211}\text{Bi}$ . On the other hand,  $^{213}\text{Bi}$ , which is a decay product of  $^{225}\text{Ac}$ , showed, in all biological matrices, higher released activity (from 20 to 40%, except saline) which represented up to 20 percentage points more release activity than  $^{225}\text{Ac}$  during the 48 h period.

The prepared  $\alpha\text{-ZrP}$  needs to be examined further. Firstly, it is important to focus on the preparation of nanoparticles with well-defined size, secondly to try to construct additional shell structure in order to limit the activity release. It is also possible that the intrinsic labelling of NPs could prevent high release of both the  $^{223}\text{Ra}$  and  $^{225}\text{Ac}$  and their daughter progeny. At the same time, additional surface modification should possibly improve the biodistribution of the labelled NPs, which are typically picked up by the spleen and lungs.

**Acknowledgements** This work was supported by Technology Agency of the Czech Republic (TJ04000129) and Czech Technical University in Prague (SGS22/188/OHK4/3T/14). Ministry of Education, Youth and Sports of the Czech Republic, grant number CZ.02.1.01/0.0/0.0/15\_003/0000464.

**Funding** Open access publishing supported by the National Technical Library in Prague.

## Declarations

**Conflict of interest** The authors declare no conflict of interest.

**Open Access** This article is licensed under a Creative Commons Attribution 4.0 International License, which permits use, sharing, adaptation, distribution and reproduction in any medium or format, as long as you give appropriate credit to the original author(s) and the source, provide a link to the Creative Commons licence, and indicate if changes were made. The images or other third party material in this article are included in the article's Creative Commons licence, unless indicated otherwise in a credit line to the material. If material is not included in the article's Creative Commons licence and your intended use is not permitted by statutory regulation or exceeds the permitted use, you will

need to obtain permission directly from the copyright holder. To view a copy of this licence, visit <http://creativecommons.org/licenses/by/4.0/>.

## References

- Morgenstern A, Apostolidis C, Kratochwil C, Sathekge M, Krolicki L, Bruchertseifer F (2018) An overview of targeted alpha therapy with  $^{225}\text{Ac}$  and  $^{213}\text{Bi}$ . *Curr Radiopharm* 11:200–208
- Guerra Liberal FDC, O'Sullivan JM, McMahon SJ, Prise KM (2020) Targeted alpha therapy: current clinical applications. *Cancer Biother Radiopharm* 35:404–417
- Kim YS, Brechbiel MW (2012) An overview of targeted alpha therapy. *Tumour Biol* 33:573–590
- Kozempel J, Mokhodoeva O, Vlk M (2018) Progress in targeted alpha-particle therapy: what we learned about recoils release from in vivo generators. *Molecules* 23:581
- Majkowska-Pilip A, Gawęda W, Żelechowska-Matysiak K, Wawrowicz K, Bilewicz A (2020) Nanoparticles in targeted alpha therapy. *Nanomaterials* 10:1366
- De Kruijff RM, Wolterbeek HT, Denkova AG (2015) A critical review of alpha radionuclide therapy—how to deal with recoiling daughters? *Pharmaceuticals* 8:321–336
- Suchánková P, Kukleva E, Štamberg K, Nykl P, Sakmár M, Vlk M, Kozempel J (2015) Determination, modeling and evaluation of kinetics of  $^{223}\text{Ra}$  sorption on hydroxyapatite and titanium dioxide nanoparticles. *Materials* 2020:13
- Mokhodoeva O, Vlk M, Malkova E, Kukleva E, Micolova P, Štamberg K, Šlouf M, Dzhaneloda R, Kozempel J (2016) Study of  $^{223}\text{Ra}$  uptake mechanism by  $\text{Fe}_3\text{O}_4$  nanoparticles: towards new prospective theranostic SPIONs. *J Nanopart Res* 18:301–313
- Piotrowska A, Leszczuk E, Bruchertseifer F, Morgenstern A, Bilewicz A (2013) Functionalized NaA nanozeolites labeled with  $^{224,225}\text{Ra}$  for targeted alpha therapy. *J Nanopart Res* 15:2082
- Kazakov AG, Garashchenko BL, Yakovlev RY, Vinokurov SE, Kalmykov SN, Myasoedov BF (2020) An experimental study of sorption/desorption of selected radionuclides on carbon nanomaterials: a quest for possible applications in future nuclear medicine. *Diam Relat Mater* 104:107752
- Bilewicz A, Cędrowska E, Gawęda W, Bruchertseifer F, Morgenstern A (2019) Barium ferrite magnetic nanoparticles labeled with Ra-223: a new potential magnetic radiobioconjugate for targeted alpha therapy. *J Label Compd Radiopharm* 62:103
- Clara JA, Monge C, Yang YZ, Takebe N (2020) Targeting signaling pathways and the immune microenvironment of cancer stem cells—a clinical update. *Nat Rev Clin Oncol* 17:204–232
- Chang MY, Seideman J, Sofou S (2008) Enhanced loading efficiency and retention of  $^{225}\text{Ac}$  in rigid liposomes for potential targeted therapy of micrometastases. *Bioconjug Chem* 19:1274–1282
- Salvanou EA, Stellas D, Tsoukalas C, Mavroidi B, Paravatou-Petsotas M, Kalogeropoulos N, Xanthopoulos S, Denat F, Laurent G, Bazzi R et al (2020) A proof-of-concept study on the therapeutic potential of Au nanoparticles radiolabeled with the alpha-emitter actinium-225. *Pharmaceutics* 12:188
- Cędrowska E, Pruszyński M, Majkowska-Pilip A, Męczyńska-Wielgosz S, Bruchertseifer F, Morgenstern A, Bilewicz A (2018) Functionalized  $\text{TiO}_2$  nanoparticles labelled with  $^{225}\text{Ac}$  for targeted alpha radionuclide therapy. *J Nanopart Res* 20:83
- Woodward J, Kennel SJ, Stuckey A, Osborne D, Wall J, Rondinone AJ, Standaert RF, Mirzadeh S (2011)  $\text{LaPO}_4$  nanoparticles doped with actinium-225 that partially sequester daughter radionuclides. *Bioconjug Chem* 22:766–776
- González MT, Dame AN, Mirzadeh S, Rojas JV (2019) Gadolinium vanadate nanocrystals as carriers of  $\alpha$ -emitters ( $^{225}\text{Ac}$ ,  $^{227}\text{Th}$ ) and contrast agents. *J Appl Phys* 125:214901
- Mulvey JJ, Villa CH, McDevitt MR, Escorcía FE, Casey E, Scheinberg DA (2013) Self-assembly of carbon nanotubes and antibodies on tumours for targeted amplified delivery. *Nat Nanotechnol* 8:763–771
- Xiao H, Liu S (2018) Zirconium phosphate (ZrP)-based functional materials: synthesis. *Prog Appl Mater Des* 155:19–35
- Wiikinkoski EW, Harjula RO, Lehto JK et al (2017) Effects of synthesis conditions on ion exchange properties of  $\alpha$ -zirconium phosphate for Eu and Am. *Radiochim Acta* 105:1033–1042
- NuDat 3.0 [Cited 6.11.2022]. <https://www.nndc.bnl.gov/nudat3/>
- Ondrák L, Fialová K, Sakmár M, Vlk M, Štamberg K, Drtinová B, Šlouf M, Bruchertseifer F, Morgenstern A, Kozempel J (2022) Preparation and characterization of  $\alpha$ -zirconium phosphate as a perspective material for separation of medicinal radionuclides

**Publisher's Note** Springer Nature remains neutral with regard to jurisdictional claims in published maps and institutional affiliations.